

# 1 Reverse microemulsion synthesis of layered gadolinium hydroxide 2 nanoparticles

3

4 Yadong Xu,<sup>a</sup> Jugal Suthar,<sup>a</sup> Raphael Egbu,<sup>a</sup> Andrew J. Weston,<sup>a</sup> Andrew M. Fogg,<sup>b,\*</sup> and Gareth R.  
5 Williams<sup>a\*</sup>

6

7 <sup>a</sup>UCL School of Pharmacy, University College London, London, WC1N 1AX, UK

8 <sup>b</sup> Department of Chemical Engineering, University of Chester, Thornton Science Park, Cheshire, CH2  
9 4NU, UK

10 \* Authors for correspondence. Email: [a.fogg@chester.ac.uk](mailto:a.fogg@chester.ac.uk) (AMF); [g.williams@ucl.ac.uk](mailto:g.williams@ucl.ac.uk) (GRW). Tel:  
11 +44 (0) 1244 512516 (AMF); +44(0) 207 753 5868 (GRW)

12

13

## 14 Abstract

15 A reverse microemulsion approach has been explored for the synthesis of layered gadolinium  
16 hydroxide (LGdH) nanoparticles in this work. This method uses oleylamine as a multifunctional agent,  
17 acting as surfactant, oil phase and base. 1-butanol is additionally used as a co-surfactant. A  
18 systematic study of the key reaction parameters was undertaken, including the volume ratio of  
19 surfactant (oleylamine) to water, the reaction time, synthesis temperature, and the amount of co-  
20 surfactant (1-butanol) added. It proved possible to obtain pristine LGdH materials at temperatures of  
21 120 °C or below with an oleylamine : water ratio of 1:4. Using larger amounts of surfactant or higher  
22 temperatures caused the formation of Gd(OH)<sub>3</sub>, either as the sole product or as a major impurity  
23 phase. The LGdH particles produced have sizes of ca. 200 nm, with this size being largely  
24 independent of temperature or reaction time. Adjusting the amount of 1-butanol co-surfactant  
25 added permits the size to be varied between 200 and 300 nm.

## 26 Keywords

27 Layered gadolinium hydroxide; reverse microemulsion; nanoparticles; oleylamine

28

## 291. Introduction

30 Ion-exchangeable layered materials have attracted widespread attention for a broad range of  
31 applications. Materials able to exchange both cations and anions are known [1], with the latter  
32 having been more widely studied [2, 3]. In both cases, the incorporation of guest ions into the  
33 interlayer space of the host materials can have a number of benefits: for instance, the stability of  
34 guest species can be improved by intercalation [4, 5].

35

36 One family of materials which has been particularly extensively studied is the layered double  
37 hydroxides (LDHs) [2]. LDHs comprise positively-charged mixed-metal hydroxide layers, with charge-  
38 balancing anions in the interlayer region [2]. A large variety of inorganic and organic anions can be  
39 incorporated into their interlayer space by ion-exchange reactions [6-8]. This rich intercalation  
40 chemistry has been extensively exploited: LDHs have been investigated for applications such as flame  
41 retardants [9, 10], catalysts and catalyst precursors [11], CO<sub>2</sub> adsorbents [12-16], cement additives  
42 [17] and drug delivery systems [7, 18-20]. Bioactive molecules have been intercalated into the  
43 interlayer space of LDHs on a number of occasions. Examples include non-steroidal anti-  
44 inflammatory drugs such as naproxen, diclofenac, gemfibrozil, ibuprofen and 2-propylpenpenoic acid  
45 [7, 19]. There are also reports of the encapsulation of anticancer drugs (e.g. 5-fluorouracil and  
46 methotrexate) [21, 22]. LDH-drug intercalates have been found to lead to sustained drug release  
47 profiles and reduced side effects compared to the free drug [7, 19].

48

49 Beyond LDHs, there exists a range of alternative layered materials capable of anion exchange. These  
50 include the recently reported layered rare-earth hydroxides (LRHs). There are a range of LRHs  
51 possible, but those capable of anion exchange have the general formula  $[R_2(OH)_5]^+(A^n)_{1/n} \cdot yH_2O$   
52 (where  $R = Ln^{3+}$ ,  $A^n =$  an anion, and  $1 \leq y \leq 2$ ). LRHs contain lanthanide cations and hydroxide ions in  
53 their positively charged layers, and charge-balancing anions in the interlayer region [23-25]. Typical  
54 examples include  $[Gd_2(OH)_5]Cl \cdot 1.5H_2O$  and  $[Yb_2(OH)_5]Cl \cdot 1.5H_2O$  [3]. The inorganic anions typically  
55 present in the gallery of LRHs immediately after synthesis can be readily replaced by other inorganic  
56 or organic species such as azamacrocyclic crown ether [26], or amino acids [27].

57

58 LRHs could thus be potent alternatives to LDHs for use as, for instance, drug delivery systems.  
59 Moreover, LRHs possess the magnetic and fluorescent properties of the rare-earth metals they  
60 contain, which could give additional benefits. The combination of ion exchange intercalation  
61 chemistry and rare earth elements in the layers can lead to integrated materials with many  
62 applications in medical science [28, 29], catalysis [30], separation science [26], sensor technologies

63[31], and luminescence devices [5, 27, 32-40]. Some studies have focused on incorporating  
64sensitizers or quenchers to tune the colour emission of LRH hybrids, for instance [3, 5, 27].

65

66Magnetic resonance imaging (MRI) is a technique widely used in biomedical imaging. It is popular in  
67part because it does not use radioactive agents or high-energy electromagnetic waves, and has high  
68spatial and temporal resolution [41]. To obtain good quality images, however, the patient must be  
69administered what is termed a “contrast agent”, a chemical entity used to enhance the quality of the  
70images obtained and permit accurate diagnoses. Commercial contrast agents are commonly based  
71on  $Gd^{3+}$ . This is because the electronic relaxation time of  $Gd^{3+}$  is very long and it has a high number of  
72unpaired electrons, which means that it can enhance both the longitudinal ( $r_1$ ) and transverse ( $r_2$ )  
73relaxation times of water protons [42]. Free  $Gd^{3+}$  is extremely toxic, and thus the agents used in the  
74clinic are based on chelation complexes designed to ensure that the Gd present remains complexed  
75at all times. An alternative route to preclude free  $Gd^{3+}$  getting into solution is to incorporate it into an  
76inorganic matrix, and hence layered gadolinium hydroxides (LGdHs) might be viable contrast agents  
77[43]. The potential of LGdHs in this regard has been explored in several reports [28, 29, 43, 44], and  
78the results obtained are promising. The LGdH matrix has also attracted a little attention for use as a  
79drug delivery system, with the intercalation of several pharmaceutically active molecules including  
80antibiotics, amino acids, and microRNA [43, 45].

81

82Control of particle size can be extremely important to achieve the desired results *in vivo*, and for this  
83reason much attention has been paid in particular to the production of nanoscale materials, which  
84have been explored in many fields [46]. The size of LDH particles has been shown to play an  
85important role in their interactions with cells, for instance [47]. Therefore, controlling the particle  
86size of LGdH will be important to ensure uptake by cells, and thus to improve its performance in MRI  
87applications. However, little effort has been applied to the synthesis of LRH nanoparticles to date.

88

89One route to control particle size is the use of reverse microemulsion systems. These comprise water  
90droplets dispersed in an oil continuous phase; when materials are grown from an aqueous solution,  
91performing the reaction in such systems means that the particle size is controlled by the size of the  
92droplets, so long as that the emulsion is stable and there is no coalescence. This approach has been  
93found to lead to high degrees of control over particle size, morphology, geometry, and surface area  
94[46], and microemulsion systems have emerged as an effective approach to synthesize nanomaterials  
95such as metallic catalysts [48], semiconductors [49], ceramics [50], and silica [51]. Here, we apply this  
96approach for the first time to the synthesis of nanosized LGdH materials, aiming to produce particles

97with sizes suitable for cellular uptake. We report the synthesis of LGdH nanoparticles using a method  
98in which oleylamine acts as oil phase, base and surfactant, permitting an extremely simple  
99microemulsion formulation to be employed.

100

## 1012 **Experimental**

### 1022.1 **Materials**

103Oleylamine and 1-butanol were purchased from Sigma-Aldrich (Gillingham, UK), while gadolinium  
104chloride hexahydrate was supplied by Alfa Aesar (Heysham, UK). All water used was deionized, and  
105all other chemicals were of analytical grade and used without further purification.

106

### 1072.2 **Methods**

#### 1082.2.1 **General protocol**

109A novel reverse microemulsion method which employs oleylamine as oil phase, base and surfactant  
110was developed in 2012 to synthesize LDHs [47]. Experiments were carried out following this method  
111with minor modifications. A 0.5 M solution of  $GdCl_3 \cdot 6H_2O$  in deionized water was first prepared, and  
112to this a mixture of oleylamine and 1-butanol was added dropwise with vigorous stirring. After 10  
113min of constant stirring, the resultant mixture was transferred to a Teflon-lined stainless steel  
114autoclave (23 mL) and treated hydrothermally. The resulting precipitates were collected by  
115centrifugation, washed with a mixture of water and ethanol (1:1, v/v), and dried at 40 °C for one day.

116

#### 1172.2.2 **Optimization**

118A detailed optimization process was undertaken in this work. First, since the volume ratio of  
119surfactant to water is known to be a determining factor for particle size [47, 52], a range of  
120oleylamine : water ratios were explored (4:1, 3:2, 1:3 and 1:4). Specifically, 8, 6, 2.5 or 2 mL of  
121oleylamine was first combined with 5 mL of 1-butanol. The resultant mixtures were added to 2, 4, 7.5  
122or 8 mL of a 0.5 M Gd chloride solution. The total volume of oleylamine and water was kept at 10 mL,  
123and the total solution volume in the autoclave was 15 mL. Hydrothermal treatment was undertaken  
124at 120 °C for 18 h. The resulting samples are denoted as LGdH- $O_m$ - $W_n$  ( $m$  = volume of oleylamine,  $n$ =  
125volume of water).

126

127Second, the temperature was optimized. With an increase in temperature in a hydrothermal process,  
128the particle size of the product tends to be larger [51]; however, high temperatures could also lead to  
129potential degradation or phase transformation. The surfactant to water volume ratio was set to 1:4,  
130and each reaction mixture comprised 2 mL oleylamine, 5 mL 1-butanol, and 8 mL Gd chloride

131solution. Hydrothermal treatments were carried out at temperatures ranging from 90 °C to 150 °C for  
13218 h. The products are denoted LGdH-90 °C, LGdH-120 °C, and LGdH-150 °C.

133Third, the aging duration is another factor which could determine the particle size: the longer the  
134crystals grow, the larger they will be. A volume ratio of surfactant to water of 1:4 was used, and again  
135each reaction mixture comprised 2 mL oleylamine, 5 mL 1-butanol, and 8 mL Gd chloride solution.  
136LGdH nanoparticles were prepared with hydrothermal treatment at 12 h, 18 h or 24 h at 120 °C. The  
137products were named LGdH-12h, LGdH-18h, and LGdH-24h.

138Finally, the co-surfactant amount in water-in-oil microemulsion systems has been reported to have  
139an important effect on particle growth, with nanoparticle size rising with an increasing amount of co-  
140surfactant [51]. Hence, the volume of 1-butanol was varied from 3 to 9 mL. The ratio of surfactant to  
141water was fixed at 1:4, so each reaction mixture comprised 2 mL of oleylamine, 8 mL of Gd chloride  
142solution, and between 3 and 9 mL of 1-butanol. Experiments were carried out at 120 °C for 12 h. The  
143materials obtained were designated LGdH-3mL, LGdH-5mL, LGdH-7mL and LGdH-9mL.

## 144**2.3 Characterization**

### 145**2.3.1 X-ray diffraction (XRD)**

146Power XRD patterns were recorded over the  $2\theta$  range from 3 to 45° on a Rigaku MiniFlex 600  
147diffractometer (Tokyo, Japan), using Cu K $\alpha$  radiation ( $\lambda = 1.5418 \text{ \AA}$ ) at 40 kV and 15 mA.

### 148**2.3.2 Fourier transform infrared (FTIR) spectroscopy**

149Infrared spectra were obtained using a Spectrum 100 FTIR spectrometer (Perkin Elmer, Waltham,  
150MA, USA) over the range 650–4000  $\text{cm}^{-1}$  with a resolution of 2  $\text{cm}^{-1}$ .

### 151**2.3.3 Dynamic light scattering (DLS)**

152Dynamic light scattering measurements were performed on a Zetasizer Nano ZS instrument (Malvern  
153Instruments, Malvern, UK). 1-2 mg of LGdH nanoparticles was suspended in ethanol and sonicated  
154for ca. 15 min prior to measurements.

### 155**2.3.4 Transmission electron microscopy (TEM)**

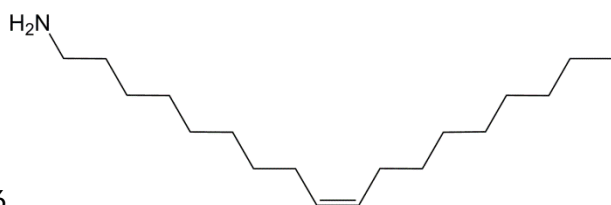
156LGdH nanoparticles (5 mg) were dispersed in ethanol (1 mL), followed by 20 minutes of sonication. A  
157few drops of each suspension were then placed onto a lacey carbon coated copper grid, and ethanol

158allowed to evaporate. TEM was performed using a FEI CM120 Bio Twin microscope (Philips,  
159Amsterdam, Netherlands) with an accelerating voltage of 120 kV.

160

### 1613. Results

162The synthesis of LGdH nanoparticles was first attempted using a previously explored protocol in  
163which Triton X-100, 2,2,4-trimethylpentane and 1-butanol act as surfactant, oil phase and co-  
164surfactant [53]. However, this method was time-consuming (3 days) and suffered from low yields. In  
165addition, the obtained nanoparticles were of very low crystallinity (ascribed to stacking defects), and  
166had a wide range of sizes (from tens of nanometers to several micrometers). Replacing 1-butanol  
167with propan-2-ol had no significant effect on the findings. This route was thus deemed unsuitable.  
168We then turned to an alternative literature protocol. Wang and O'Hare [47] have reported an  
169approach using oleylamine (Figure 1) as a multi-functional agent which acts as the oil phase, base,  
170and surfactant simultaneously. Alkaline conditions are provided as a result of the amine group, and  
171the amine head group along with its alkyl chain tail acts as a surfactant. This leads to the formation  
172of reverse micelles in a water-in-oil system. 1-butanol was also added as a co-surfactant, separating  
173the oleylamine units and reducing the repulsive forces between the protonated head groups [47].  
174Wang and O'Hare's oleylamine method was systematically explored for the synthesis of LGdH in this  
175work.



176

177**Figure 1:** The chemical structure of oleylamine.

178

#### 1793.1 Effect of surfactant to water ratio

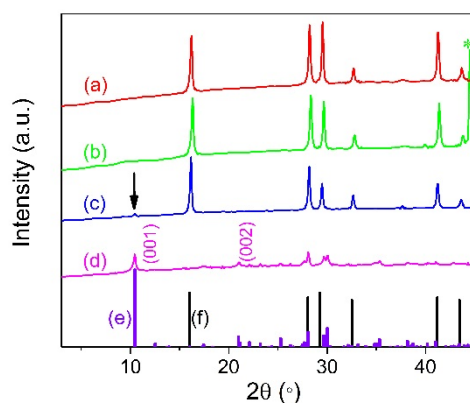
180The first reaction parameter to be investigated was the ratio of surfactant to water in the system. A  
181series of emulsions were prepared as detailed in .

182

183**Table 1:** Details of reactions performed with different ratios of oleylamine to water. All were performed at 120 °C for 18 h,  
184with 5 mL of 1-butanol added.

Sample ID	Oleylamine (mL)	volume	Aqueous volume (mL)	solution	Oleylamine/water ratio	volume
LGdH-O8-W2	8		2		4:1	
LGdH-O6-W4	6		4		3:2	
LGdH-O2.5-W7.5	2.5		7.5		1:3	
LGdH-O2-W8	2		8		1:4	

185The powder XRD patterns of the products obtained are presented in Figure 2. Phase-pure LGdH  
186nanoparticles could be synthesized only with a 1:4 volume ratio of oleylamine to water. At ratios  
187below this, the diffraction patterns very closely resemble that of Gd(OH)<sub>3</sub> (JCPDS #38-1042). At ratios  
188of 4:1 and 3:2, no lamellar (00*l*) reflections at all were observed in the XRD data. At a volume ratio of  
1891:3, a weak reflection (marked with an arrow in Figure 2) at ca. 10.5° was observed, which  
190corresponds to the (001) Bragg reflection of LGdH and indicates the presence of a small amount of  
191the LRH alongside the Gd(OH)<sub>3</sub> majority product. The pattern obtained for sample LGdH-O2-W8, with  
192a 1:4 ratio of surfactant to water, matches literature data for chloride intercalated LGdH (LGdH-Cl)  
193[54-56]. The position of the (001) Bragg reflection corresponds to an interlayer spacing of 8.48 Å, in  
194excellent agreement with previously reported values for chloride intercalates [28, 56].



195

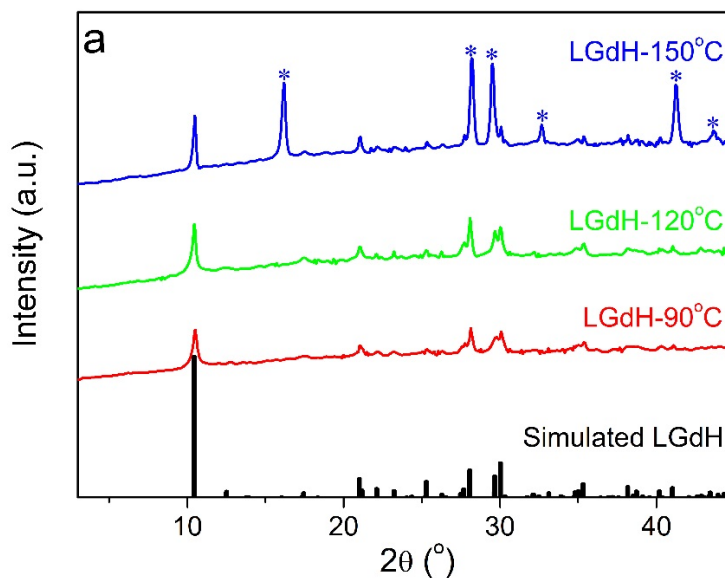
196**Figure 2:** Powder X-ray diffraction patterns of LGdH nanoparticles prepared with different volume ratios of surfactant to  
197water: (a) LGdH-O8-W2; (b) LGdH-O6-W4; (c) LGdH-O2.5-W7.5; (d) LGdH-O2-W8. The calculated reflection positions are  
198also shown for (e, purple) LGdH-Cl [56] and (f, black) Gd(OH)<sub>3</sub> [JCPDS #38-1042]. The Bragg reflection marked \* corresponds  
199to the sample holder.

200

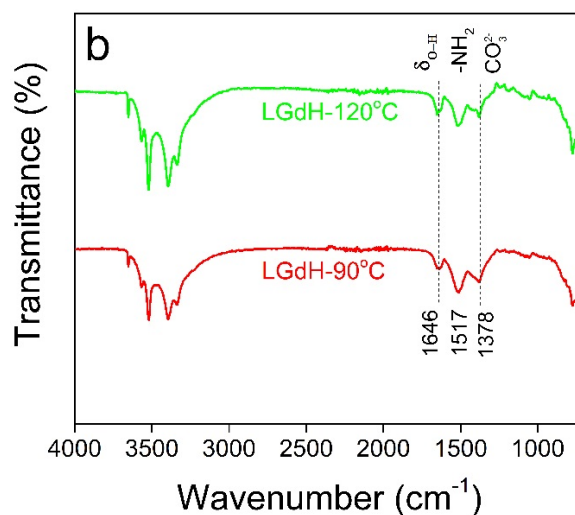
201

### 2023.2 Effect of temperature

203Data for samples prepared at different temperatures with a 1:4 surfactant to water ratio are given in  
204Figure 3.



205



206

207**Figure 3:** Experimental data for syntheses conducted at 90, 120, and 150 °C. (a) XRD patterns; and, (b) IR spectra.  
208Reflections marked with \* in (a) arise from  $\text{Gd}(\text{OH})_3$ .  
209

210The materials generated at 90, 120 and 150 °C all present basal (00 $l$ ) reflections (Figure 3), indicative  
211of an interlayer spacing of 8.42 Å. Significant amounts of  $\text{Gd}(\text{OH})_3$  can be seen in the sample  
212synthesized at 150 °C, but phase pure LGdH was successfully synthesized at 90 and 120 °C. The Bragg

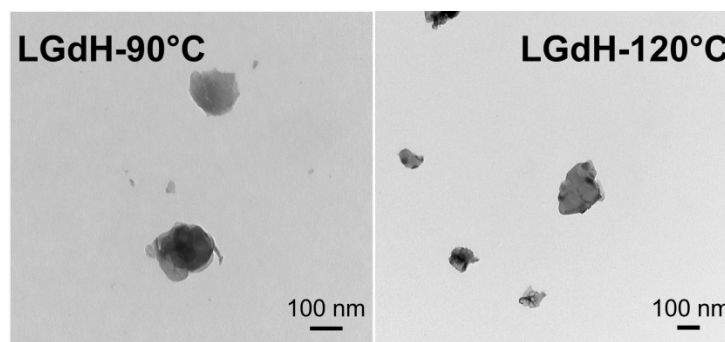
213 reflections of product from the 120 °C reaction are somewhat stronger and sharper than those of the  
 214 90 °C analogue, implying that samples heated at the higher temperature are better crystallized and  
 215 have larger crystallite sizes. IR spectra (Figure 3(b)) confirm the successful synthesis of LGdHs at 90  
 216 and 120 °C. The two spectra contain the same features, with the broad set of bands centred at ca.  
 217 3500 cm<sup>-1</sup> attributed to the stretching vibration of the OH groups from both interlayer water and the  
 218 hydroxide layers [26, 40]. The absorbance at 1646 cm<sup>-1</sup> is ascribed to the bending vibrations of the  
 219 interlayer water molecules ( $\delta_{\text{O-H}}$ ) [57]. Bands below 1000 cm<sup>-1</sup> correspond to the phonon vibrations of  
 220 the structure. The peaks at 1517 and 1378 cm<sup>-1</sup> indicate the presence of residual oleylamine, and of  
 221 some CO<sub>3</sub><sup>2-</sup> co-intercalated with the Cl<sup>-</sup> anions, respectively.

222 **Table 2:** Crystallite sizes of LGdH nanoparticles prepared at different temperatures, analyzed using the Scherrer equation ( $K$   
 223 = 0.89). \* denotes occasions where no data could be obtained.

Sample ID	FWHM (°)		Crystallite size (nm)	
	(001)	(220)	c-direction	ab-plane
LGdH-90°C	0.339	0.318	24.6	27.1
LGdH-120°C	0.247	*	35.3	*

224

225 The LGdH patterns can be indexed in orthorhombic symmetry, and hence the (001) Bragg reflection  
 226 can be applied to estimate the crystallite size along the c-axis (the thickness of the particles), while  
 227 the (220) reflection can be used to estimate the crystallite size in the ab plane. The values estimated  
 228 using the Scherrer equation are summarized in Table 2. The crystallite size in the c-direction is found  
 229 to be around 25 - 35 nm, with a comparable size in the ab-plane where this could be determined.  
 230 TEM images (Figure 4) show both LGdH-90°C and LGdH-120°C to comprise small aggregates of  
 231 platelets, with lateral sizes between around 100 and 200 nm. The primary particle size is perhaps  
 232 somewhat larger than the size obtained from Scherrer analysis (as would be expected given the  
 233 assumptions involved in applying the latter), but overall the two sets of data are consistent.

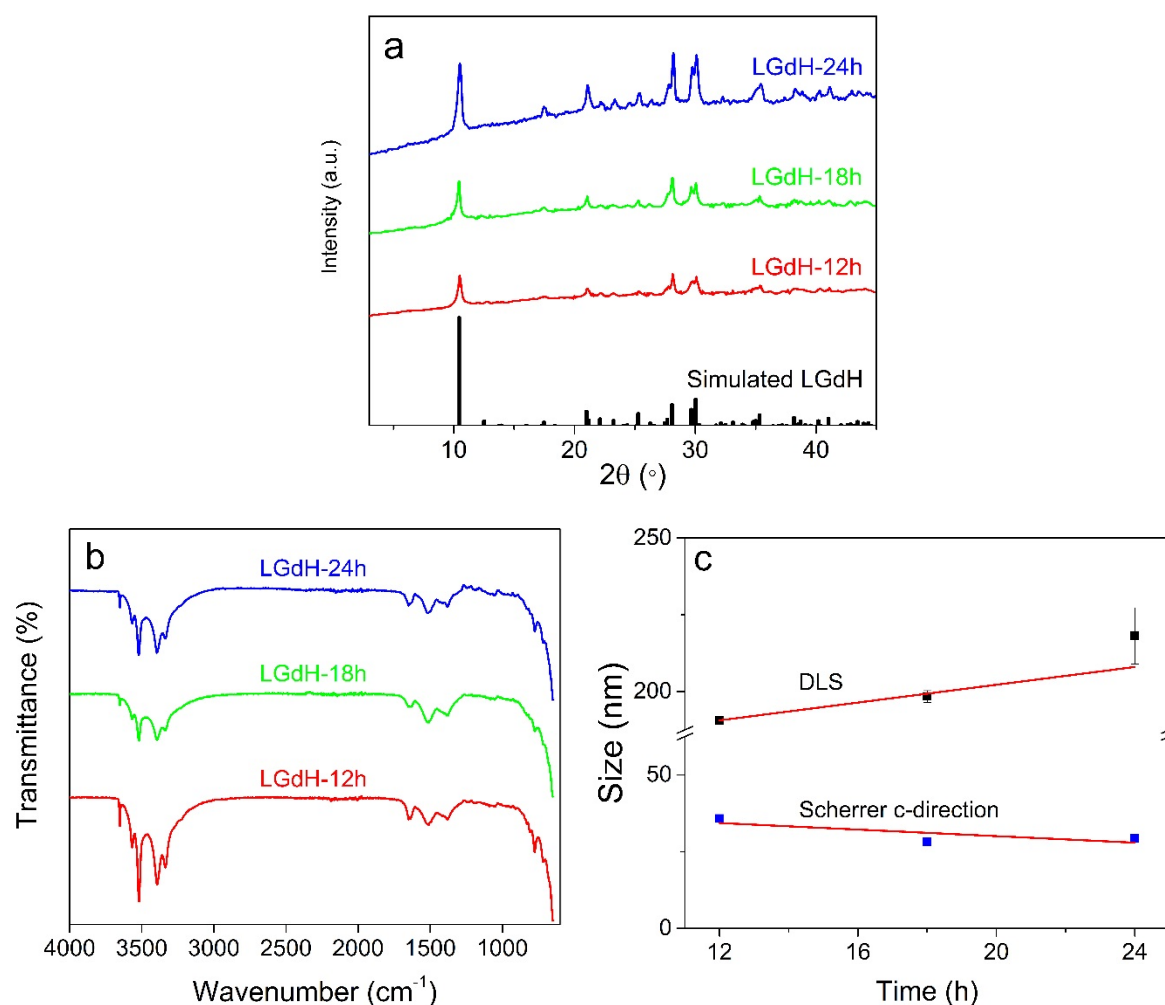


234

235 **Figure 4:** TEM images of LGdH prepared at different temperatures.

### 2373.3 Effect of time

238The volume ratio of oleylamine to water and heating temperature were fixed at 1:4 and 90 °C, while  
 239the aging time was varied from 12 to 24 h. XRD patterns of the products are given in Figure 5(a). The  
 240presence of a series of (00l) basal reflections in each case indicates the formation of lamellar  
 241structures. The interlayer spacing of all three samples is around 8.45 Å, consistent with the literature  
 242for LGdH-Cl materials [28, 56]. Scherrer analysis of the (001) and (220) reflections (see 120°C.)  
 243reveals that the crystallite size in the ab plane seems to increase with reaction time, but that in the c-  
 244diameter is largely constant, with possibly a decrease in size after reaction times longer than 12 h.  
 245The IR spectra (Figure 5(b)) are analogous to those discussed previously in terms of the peak  
 246positions (see discussion of Figure 3(b)).



247**Figure 5:** Data on the LGdH products obtained after different reaction times. (a) XRD patterns; (b) IR spectra; and, (c)  
 248particle size data.

249

250DLS measurements were employed to determine the hydrodynamic particle size (120°C.). There  
 251appears to be a trend to larger particles with longer reaction times (Figure 5(c)). TEM data are

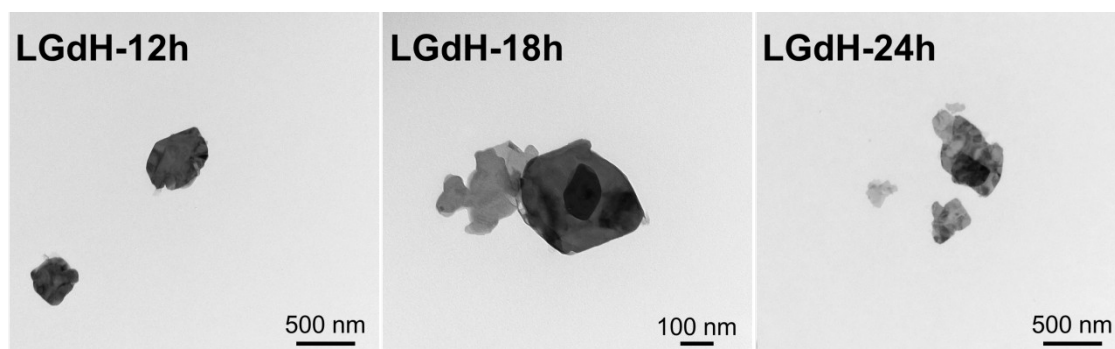
252 presented in Figure 6. For each of LGdH-12h, LGdH-18h and LGdH-24h the samples comprise small  
 253 aggregates of platelets, with sizes roughly in the ranges 250 – 500 nm, 300 – 700 nm, and 250 – 750  
 254 nm respectively. These sizes are rather larger than those observed in DLS, which is ascribed to  
 255 aggregation occurring during the TEM sample preparation process, but in general support the idea of  
 256 larger particles forming with increased reaction times. However, the differences observed are slight,  
 257 and overall it appears that the reaction time has little effect on the particle size.

258 The LGdH-18h sample was prepared under the same conditions as the LGdH-120°C sample discussed  
 259 in Section 3.2 and shown in Figure 4. The c-direction crystallite sizes, as determined through the  
 260 Scherrer equation, are comparable for the two samples (28.2 nm for LGdH-18h, cf. 35.3 nm for LGdH-  
 261 120°C), but the TEM particle sizes are somewhat different. This is ascribed to the propensity of the  
 262 particles to aggregate, and the presence of different size secondary particles in the different samples  
 263 imaged. A comparison of Figure 4 and Figure 6 reveals that the primary particle sizes are similar in  
 264 both, and the DLS particle size for LGdH-18h agrees well with the TEM estimate of particle size for  
 265 LGdH-120°C.

266 **Table 3:** Summary of particle size data for LGdH obtained after 12, 18, and 24h. \* denotes occasions where no data could be  
 267 obtained.

Sample ID	c-direction	ab-plane crystallite		
	crystallite size (nm)	size (nm)	Mean	SD
LGdH-12h	28.2	20.2	108	1.0
LGdH-24h	28.4	21.7	219	0.2

268



269

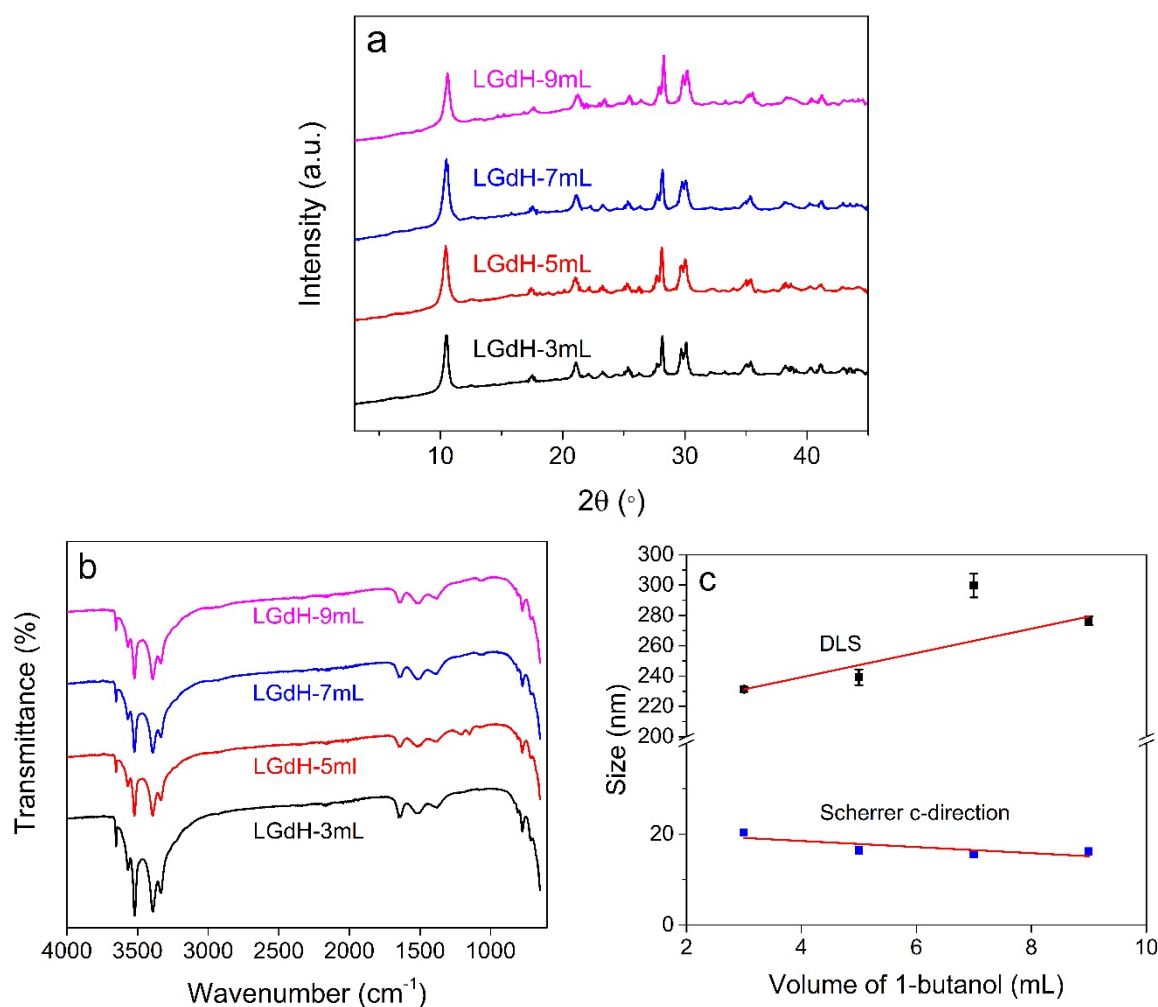
270 **Figure 6:** TEM images of LGdH-12h, LGdH-18h, and LGdH-24h.

271

### 272 3.4 Effect of co-surfactant

273 The literature reports that the particle size of silica nanospheres prepared by a microemulsion  
 274 method decreased as the amount of co-surfactant decreased [51]. Therefore, the amount of 1-  
 275 butanol used in the synthesis was varied in attempts to tune the nanoparticle size. The products' XRD

276 patterns (Figure 7(a)) all contain the characteristic basal (001) reflections of layered LGdH particles,  
 277 with (001) reflections at ca.  $10.5^\circ$  and (002) at ca.  $21.1^\circ$ . The weak reflections between the (001) and  
 278 (002) reflections indicate the well-ordered in-plane structure of the LGdH materials. Scherrer analysis  
 279 of the data (Table 4) does not reveal any clear relationship between the amount of co-surfactant and  
 280 crystallite size. LGdH-3mL has the largest crystallites in the c-direction, but the non-basal reflections  
 281 are too broad to permit measurement of their FWHM values. The other three materials have  
 282 essentially the same crystallite size in the c-direction, and a small amount of variation in the ab  
 283 plane, with LGdH-7mL presenting the smallest value for the latter.



284 **Figure 7:** The effect of changing the co-surfactant volume on LGdH synthesis. (a) XRD patterns; (b) IR spectra; and, (c)  
 285 particle size data.

286 The IR spectra (Figure 7(b)) show the same absorbance peaks as discussed previously, corresponding  
 287 to -OH,  $\text{-NH}_2$  and  $\text{CO}_3^{2-}$  and confirming the formation of LGdH materials. Hydrodynamic diameters  
 288 were measured by DLS (Table 4), and their relationship with the 1-butanol volume is presented in  
 289 Figure 7(c). As the amount of co-surfactant increases, there is a general trend for the diameter of the  
 290 LGdH nanoparticles to increase. This agrees with the literature findings for hollow silica nanoparticles

291[51]. However, this trend is not completely clear, and it also apparent that there is some batch-to-  
 292batch variation in the sizes: LGdH-5mL was prepared under identical synthetic conditions to LGdH-  
 29312h, but the two have somewhat different sizes both in terms of XRD crystallite sizes and DLS particle  
 294sizes. Thus, although it seems that using larger amounts of co-surfactant can help to increase the  
 295particle size produced a little, this effect is not hugely pronounced. TEM images were obtained on  
 296LGdH-3mL and LGdH-5mL (data not shown), and both found to be very similar. The samples comprise  
 297aggragrates of platelets, with sizes in the region of 100 – 300 nm.

298**Table 4:** Summary of the particle sizes of LGdH obtained with 3, 5, 7, and 9 mL of 1-butanol. \* denotes that values could not  
 299be obtained.

Sample ID	c-direction		ab-plane crystallite	
	crystallite size (nm)	size (nm)	Mean	SD
LGdH 5ml	16.4	44.1	220	5.2
LGdH 7ml	15.6	27.2	200	7.9
LGdH 9ml	16.9	47.4	277	9.9

300

#### 3014. Discussion

302The effect of the surfactant to water ratio [58], reaction temperature, reaction time and the amount  
 303of co-surfactant [51] used for the reverse microemulsion synthesis of LGdH have been systematically  
 304investigated in this work. We find that the surfactant : water ratio and the reaction temperature must  
 305be carefully controlled to ensure that the desired product is formed phase-pure; the use of excessive  
 306amounts of surfactant (> 1:4 surfactant : water ratio) or temperatures above 120 °C lead to the  
 307formation of Gd(OH)<sub>3</sub>, either phase-pure or as a major impurity. With a 1:4 ratio and temperatures of  
 308120 °C or below, however, LGdH can be obtained phase-pure. The reaction time and co-surfactant  
 309volume have some effect on particle size, but in all cases the sizes are found to be between 200 and  
 310300 nm.

311

312It is reported that as the ratio of surfactant to water increases, the microemulsion droplets tend to  
 313become smaller. If the reaction is confined to the aqueous phase, as is the case here, this should lead  
 314to smaller particles being generated [46, 58]. LGdH particle size cannot be controlled in this way in  
 315the oleylamine/1-butanol system however, because gadolinium hydroxide is found to form with high  
 316ratios. Our findings are thus in conflict with the literature on LDH materials [47]. This is because LDHs  
 317are typically synthesized at ca. pH 9 – 10, while LGdHs are prepared at ca. pH 6.7 – 7.2 [54, 59].  
 318Oleylamine acts both as base and surfactant, and the transformation of LGdH to Gd(OH)<sub>3</sub> presumably  
 319arises due to the increasingly strong alkaline environment as the oleylamine content of the system is  
 320increased. This problem does not occur with the previously-reported LDH synthesis using oleylamine

321because of the fact that LDHs are more stable at high pHs. Therefore, the LDH nanoparticle size can  
322be controlled, and reduced to as little as 49 nm by tuning the surfactant to water volume ratios [47].

323

## 3245. Conclusions

325Layered gadolinium hydroxide (LGdH) nanoparticles have been successfully synthesized by employing  
326a novel reverse microemulsion method. Pristine LGdH materials were obtained at temperatures  
327below 150 °C with an oleylamine : water ratio of 1:4. Control of particle size is difficult, however.  
328Attempts to achieve this by using more surfactant and increasing the reaction temperature were  
329unsuccessful because of the propensity of Gd(OH)<sub>3</sub> to form. It was found that at 120 °C and below  
330the temperature and the duration of heating have little effect on the size distribution, producing  
331particles around 200 nm. Varying the amount of co-surfactant (1-butanol) used allowed the size to be  
332increased from ca. 200 nm to 300 nm, with use of more butanol giving larger particles. Overall,  
333microemulsions have proved to be an effective and efficient way to synthesized LGdH nanoparticles  
334of 200 – 300 nm in size, but in order to obtain more control over particle size alternative surfactants  
335should be investigated.

336

## 3376. Acknowledgements

338The authors gratefully thank Mr David McCarthy and Mrs Kate Keen for assistance with obtaining  
339TEM images. JS and RE thank the EPSRC for the provision of PhD studentships under the Centre for  
340Doctoral Training in Advanced Therapeutics & Nanomedicines (EP/L01646X/1).

341

## 3427. References [Endnote has gone crazy, but will sort the refs out before 343we resubmit!]

344 [1] M. Ranocchiari, J.A. van Bokhoven, Catalysis by metal–organic frameworks: fundamentals and  
345 opportunities, *Phys. Chem. Chem. Phys.* 13(14) (2011) 6388-6396.

346 [2] D.O.H. Qiang Wang, Recent Advances in the Synthesis and Application of Layered Double Hydroxide (LDH)  
347 Nanosheets, *Chemical reviews* 12 (2012) 4124-4155.

348 [3] F. Geng, R. Ma, T. Sasaki, Anion-exchangeable layered materials based on rare-earth phosphors: unique  
349 combination of rare-earth host and exchangeable anions, *Acc. Chem. Res.* 43(9) (2010) 1177-1185.

350 [4] S. Takagi, D.A. Tryk, H. Inoue, Photochemical energy transfer of cationic porphyrin complexes on clay  
351 surface, *J. Phys. Chem. B* 106(21) (2002) 5455-5460.

352[5] N. Chu, Y. Sun, Y. Zhao, X. Li, G. Sun, S. Ma, X. Yang, Intercalation of organic sensitisers into layered europium  
353 hydroxide and enhanced luminescence property, *Dalton Trans* 41(24) (2012) 7409-14.

354 [6] Q. Qin, J. Wang, T. Zhou, Q. Zheng, L. Huang, Y. Zhang, P. Lu, A. Umar, B. Louis, Q. Wang, Impact of organic  
355 interlayer anions on the CO<sub>2</sub> adsorption performance of Mg-Al layered double hydroxides derived mixed  
356 oxides, *Journal of Energy Chemistry* 26(3) (2017) 346-353.

357 [7] V. Rives, M. del Arco, C. Martín, Intercalation of drugs in layered double hydroxides and their controlled  
358 release: A review, *Appl. Clay Sci.* 88-89 (2014) 239-269.

359 [8] G.R. Williams, D. O'Hare, Towards understanding, control and application of layered double hydroxide  
360 chemistry, *Journal of Materials Chemistry* 16(30) (2006) 3065.

361 [9] C. Nyambo, P. Songtipya, E. Manias, M.M. Jimenez-Gasco, C.A. Wilkie, Effect of MgAl-layered double  
362 hydroxide exchanged with linear alkyl carboxylates on fire-retardancy of PMMA and PS, *J. Mater. Chem.* 18(40)  
363 (2008) 4827-4838.

364 [10] C. Manzi-Nshuti, J.M. Hossenlopp, C.A. Wilkie, Comparative study on the flammability of polyethylene  
365 modified with commercial fire retardants and a zinc aluminum oleate layered double hydroxide, *Polym. Degr.*  
366 *Stab.* 94(5) (2009) 782-788.

367 [11] X. Xu, R. Lu, X. Zhao, S. Xu, X. Lei, F. Zhang, D.G. Evans, Fabrication and photocatalytic performance of a Zn  
368 x Cd 1- x S solid solution prepared by sulfuration of a single layered double hydroxide precursor, *Appl. Catal. B*  
369 102(1) (2011) 147-156.

370 [12] Q. Wang, J. Luo, Z. Zhong, A. Borgna, CO<sub>2</sub> capture by solid adsorbents and their applications: current  
371 status and new trends, *Energy Env. Sci.* 4(1) (2011) 42-55.

372 [13] Q. Wang, H.H. Tay, D.J.W. Ng, L. Chen, Y. Liu, J. Chang, Z. Zhong, J. Luo, A. Borgna, The effect of trivalent  
373 cations on the performance of Mg-M-CO<sub>3</sub> layered double hydroxides for high-temperature CO<sub>2</sub> capture,  
374 *ChemSusChem* 3(8) (2010) 965-973.

375 [14] Q. Wang, Z. Wu, H.H. Tay, L. Chen, Y. Liu, J. Chang, Z. Zhong, J. Luo, A. Borgna, High temperature adsorption  
376 of CO<sub>2</sub> on Mg-Al hydrotalcite: effect of the charge compensating anions and the synthesis pH, *Catal. Today*  
377 164(1) (2011) 198-203.

378 [15] Q. Wang, H.H. Tay, Z. Guo, L. Chen, Y. Liu, J. Chang, Z. Zhong, J. Luo, A. Borgna, Morphology and  
379 composition controllable synthesis of Mg-Al-CO<sub>3</sub> hydrotalcites by tuning the synthesis pH and the CO<sub>2</sub>  
380 capture capacity, *Appl. Clay Sci.* 55 (2012) 18-26.

381 [16] Q. Song, W. Liu, C.D. Bohn, R.N. Harper, E. Sivaniah, S.A. Scott, J.S. Dennis, A high performance oxygen  
382 storage material for chemical looping processes with CO<sub>2</sub> capture, *Energy Env. Sci.* 6(1) (2013) 288-298.

383 [17] J. Plank, D. Zhimin, H. Keller, F.v. Hössle, W. Seidl, Fundamental mechanisms for polycarboxylate  
384 intercalation into C<sub>3</sub>A hydrate phases and the role of sulfate present in cement, *Cement Concrete Res.* 40(1)  
385 (2010) 45-57.

386 [18] A. Alcantara, P. Aranda, M. Darder, E. Ruiz-Hitzky, Bionanocomposites based on alginate-zein/layered  
387 double hydroxide materials as drug delivery systems, *J. Mater. Chem.* 20(42) (2010) 9495-9504.

388 [19] V. Rives, M. Del Arco, C. Martin, Layered double hydroxides as drug carriers and for controlled release of  
389 non-steroidal antiinflammatory drugs (NSAIDs): a review, *Journal of controlled release : official journal of the*  
390 *Controlled Release Society* 169(1-2) (2013) 28-39.

391 [20] L. Li, W. Gu, J. Chen, W. Chen, Z.P. Xu, Co-delivery of siRNAs and anti-cancer drugs using layered double  
392 hydroxide nanoparticles, *Biomaterials* 35(10) (2014) 3331-9.

393 [21] J.-M. Oh, S.-J. Choi, G.-E. Lee, S.-H. Han, J.-H. Choy, Inorganic drug-delivery nanovehicle conjugated with  
394 cancer-cell-specific ligand, *Adv. Funct. Mater.* 19(10) (2009) 1617-1624.

395 [22] Z. Wang, E. Wang, L. Gao, L. Xu, Synthesis and properties of Mg<sub>2</sub>Al layered double hydroxides containing 5-  
396 fluorouracil, *J. Solid State Chem.* 178(3) (2005) 736-741.

397 [23] S.A. Hindocha, L.J. McIntyre, A.M. Fogg, Precipitation synthesis of lanthanide hydroxynitrate anion  
398 exchange materials, Ln<sub>2</sub>(OH)<sub>5</sub>NO<sub>3</sub>·H<sub>2</sub>O (Ln=Y, Eu-Er), *J. Solid State Chem.* 182(5) (2009) 1070-1074.

399 [24] L.J. McIntyre, L.K. Jackson, A.M. Fogg, Ln<sub>2</sub>(OH)<sub>5</sub>NO<sub>3</sub>·x H<sub>2</sub>O (Ln= Y, Gd- Lu): A Novel Family of Anion  
400 Exchange Intercalation Hosts, *Chem. Mater.* 20(1) (2008) 335-340.

401 [25] L. Poudret, T.J. Prior, L.J. McIntyre, A.M. Fogg, Synthesis and crystal structures of new lanthanide  
402 hydroxyhalide anion exchange materials, Ln<sub>2</sub>(OH)<sub>5</sub>X·1.5H<sub>2</sub>O (X = Cl, Br; Ln ) Y, Dy, Er, Yb), *Chem. Mater.* 20  
403 (2008) 7447-7453.

404 [26] W. Li, Q. Gu, F. Su, Y. Sun, G. Sun, S. Ma, X. Yang, Intercalation of azamacrocyclic crown ether into layered  
405 rare-earth hydroxide (LRH): secondary host-guest reaction and efficient heavy metal removal, *Inorganic*  
406 *chemistry* 52(24) (2013) 14010-7.

407 [27] Q. Gu, Y. Sun, N. Chu, S. Ma, Z. Jia, X. Yang, Intercalation of amino acids into Eu<sup>3+</sup>-doped layered  
408 gadolinium hydroxide and quenching of Eu<sup>3+</sup> luminescence, *Eur. J. Inorg. Chem.* 2012(28) (2012) 4407-4412.

409 [28] B.I. Lee, K.S. Lee, J.H. Lee, I.S. Lee, S.H. Byeon, Synthesis of colloidal aqueous suspensions of a layered  
410 gadolinium hydroxide: a potential MRI contrast agent, *Dalton transactions* (14) (2009) 2490-5.

411 [29] Y.-S. Yoon, B.-I. Lee, K.S. Lee, G.H. Im, S.-H. Byeon, J.H. Lee, I.S. Lee, Surface modification of exfoliated  
412 layered gadolinium hydroxide for the development of multimodal contrast agents for MRI and fluorescence  
413 imaging, *Adv. Funct. Mater.* 19(21) (2009) 3375-3380.

414 [30] F. Gándara, E.G. Puebla, M. Iglesias, D.M. Proserpio, N. Snejko, M.A. Monge, Controlling the structure of  
415 arenedisulfonates toward catalytically active materials, *Chem. Mater.* 21(4) (2009) 655-661.

416 [31] Y. Xiang, X.F. Yu, D.F. He, Z. Sun, Z. Cao, Q.Q. Wang, Synthesis of highly luminescent and anion-  
417 exchangeable cerium-doped layered yttrium hydroxides for sensing and photofunctional applications, *Adv.*  
418 *Funct. Mater.* 21(22) (2011) 4388-4396.

419 [32] Q. Zhu, J.-G. Li, C. Zhi, X. Li, X. Sun, Y. Sakka, D. Golberg, Y. Bando, Layered rare-earth hydroxides (LRHs) of  
420 (Y<sub>1-x</sub>Eu<sub>x</sub>)<sub>2</sub>(OH)<sub>5</sub>NO<sub>3</sub>·nH<sub>2</sub>O (x= 0-1): Structural variations by Eu<sup>3+</sup>-doping, phase conversion to oxides, and the  
421 correlation of photoluminescence behaviors, *Chem. Mater.* 22(14) (2010) 4204-4213.

422 [33] B.I. Lee, S.H. Byeon, Highly enhanced photoluminescence of a rose-like hierarchical superstructure  
423 prepared by self-assembly of rare-earth hydroxocation nanosheets and polyoxomolybdate anions, *Chemical*  
424 *communications* 47(14) (2011) 4093-5.

425 [34] Q. Zhu, J.G. Li, C. Zhi, R. Ma, T. Sasaki, J.X. Xu, C.H. Liu, X.D. Li, X.D. Sun, Y. Sakka, Nanometer-thin layered  
426 hydroxide platelets of (Y<sub>0.95</sub>Eu<sub>0.05</sub>)<sub>2</sub>(OH)<sub>5</sub>NO<sub>3</sub>·xH<sub>2</sub>O: exfoliation-free synthesis, self-assembly, and the  
427 derivation of dense oriented oxide films of high transparency and greatly enhanced luminescence, *J. Mater.*  
428 *Chem.* 21(19) (2011) 6903.

429 [35] X. Wu, J.G. Li, Q. Zhu, J. Li, R. Ma, T. Sasaki, X. Li, X. Sun, Y. Sakka, The effects of Gd<sup>3+</sup> substitution on the  
430 crystal structure, site symmetry, and photoluminescence of Y/Eu layered rare-earth hydroxide (LRH)  
431 nanoplates, Dalton transactions 41(6) (2012) 1854-61.

432 [36] Q. Gu, N. Chu, G. Pan, G. Sun, S. Ma, X. Yang, Intercalation of diverse organic guests into layered europium  
433 hydroxides - structural tuning and photoluminescence behavior, Eur. J. Inorg. Chem. 2014(3) (2014) 559-566.

434 [37] Q. Gu, F. Su, L. Ma, S. Ma, G. Sun, X. Yang, Intercalation of coumaric acids into layered rare-earth  
435 hydroxides: controllable structure and photoluminescence properties, J. Mater. Chem. C 3(18) (2015) 4742-  
436 4750.

437 [38] Q. Gu, F. Su, S. Ma, G. Sun, X. Yang, Controllable luminescence of layered rare-earth hydroxide composites  
438 with a fluorescent molecule: blue emission by delamination in formamide, Chemical communications 51(13)  
439 (2015) 2514-7.

440 [39] H. Kim, B.-I. Lee, H. Jeong, S.-H. Byeon, Relationship between interlayer anions and photoluminescence of  
441 layered rare earth hydroxides, J. Mater. Chem. C 3(28) (2015) 7437-7445.

442 [40] T. Shen, Y. Zhang, W. Liu, Y. Tang, Novel multi-color photoluminescence emission phosphors developed by  
443 layered gadolinium hydroxide via in situ intercalation with positively charged rare-earth complexes, J. Mater.  
444 Chem. C 3(8) (2015) 1807-1816.

445 [41] J. Key, J.F. Leary, Nanoparticles for multimodal in vivo imaging in nanomedicine, Int. J. Nanomedicine 9  
446 (2014) 711.

447 [42] H. Dong, S.R. Du, X.Y. Zheng, G.M. Lyu, L.D. Sun, L.D. Li, P.Z. Zhang, C. Zhang, C.H. Yan, Lanthanide  
448 nanoparticles: From design toward bioimaging and therapy, Chem. Rev. 115(19) (2015) 10725-815.

449 [43] D. Stefanakis, D.F. Ghanotakis, Synthesis and characterization of gadolinium nanostructured materials with  
450 potential applications in magnetic resonance imaging, neutron-capture therapy and targeted drug delivery, J.  
451 Nanoparticle Res. 12(4) (2010) 1285-1297.

452 [44] Y.S. Yoon, B.I. Lee, K.S. Lee, H. Heo, J.H. Lee, S.H. Byeon, I.S. Lee, Fabrication of a silica sphere with  
453 fluorescent and MR contrasting GdPO<sub>4</sub> nanoparticles from layered gadolinium hydroxide, Chemical  
454 communications 46(21) (2010) 3654-6.

455 [45] S.S. Yoo, R. Razzak, E. Bedard, L. Guo, A.R. Shaw, R.B. Moore, W.H. Roa, Layered gadolinium-based  
456 nanoparticle as a novel delivery platform for microRNA therapeutics, Nanotechnology 25(42) (2014) 425102.

457 [46] M.A. Malik, M.Y. Wani, M.A. Hashim, Microemulsion method: A novel route to synthesize organic and  
458 inorganic nanomaterials, Arabian J. Chem. 5(4) (2012) 397-417.

459 [47] C.J. Wang, D. O'Hare, Synthesis of layered double hydroxide nanoparticles in a novel microemulsion, J.  
460 Mater. Chem. 22(39) (2012) 21125.

461 [48] X. Zhang, K.-Y. Chan, Water-in-oil microemulsion synthesis of platinum-ruthenium nanoparticles, their  
462 characterization and electrocatalytic properties, Chem. Mater. 15(2) (2003) 451-459.

463 [49] C. Murray, D.J. Norris, M.G. Bawendi, Synthesis and characterization of nearly monodisperse CdE (E= sulfur,  
464 selenium, tellurium) semiconductor nanocrystallites, J. Am. Chem. Soc. 115(19) (1993) 8706-8715.

465 [50] A.J. Zarur, J.Y. Ying, Reverse microemulsion synthesis of nanostructured complex oxides for catalytic  
466 combustion, Nature 403(6765) (2000) 65-67.

467[51] C.H. Lin, J.H. Chang, Y.Q. Yeh, S.H. Wu, Y.H. Liu, C.Y. Mou, Formation of hollow silica nanospheres by reverse  
468 microemulsion, *Nanoscale* 7(21) (2015) 9614-26.

469[52] J.N. Coleman, M. Lotya, A. O'Neill, S.D. Bergin, P.J. King, U. Khan, K. Young, A. Gaucher, S. De, R.J. Smith, I.V.  
470 Shvets, S.K. Arora, G. Stanton, H.Y. Kim, K. Lee, G.T. Kim, G.S. Duesberg, T. Hallam, J.J. Boland, J.J. Wang, J.F.  
471 Donegan, J.C. Grunlan, G. Moriarty, A. Shmeliov, R.J. Nicholls, J.M. Perkins, E.M. Grieveson, K. Theuwissen, D.W.  
472 McComb, P.D. Nellist, V. Nicolosi, Two-dimensional nanosheets produced by liquid exfoliation of layered  
473 materials, *Science* 331(6017) (2011) 568-71.

474 [53] J. Rees, Synthesis, characterisation and application of layered rare-earth hydroxide nanoparticles, MChem  
475 thesis, University of Liverpool, 2012, p. 61.

476 [54] F. Gandara, J. Perles, N. Snejko, M. Iglesias, B. Gomez-Lor, E. Gutierrez-Puebla, M.A. Monge, Layered rare-  
477 earth hydroxides: a class of pillared crystalline compounds for intercalation chemistry, *Angewandte Chemie*  
478 45(47) (2006) 7998-8001.

479 [55] F. Geng, H. Xin, Y. Matsushita, R. Ma, M. Tanaka, F. Izumi, N. Iyi, T. Sasaki, New layered rare-earth  
480 hydroxides with anion-exchange properties, *Chemistry* 14(30) (2008) 9255-60.

481 [56] F. Geng, Y. Matsushita, R. Ma, H. Xin, M. Tanaka, F. Izumi, N. Iyi, T. Sasaki, General Synthesis and Structural  
482 Evolution of a Layered Family of  $\text{Ln}_8(\text{OH})_2\text{OCl}_4 \cdot n\text{H}_2\text{O}$  (Ln= Nd, Sm, Eu, Gd, Tb, Dy, Ho, Er, Tm, and Y), *J. Am.*  
483 *Chem. Soc.* 130(48) (2008) 16344-16350.

484 [57] Z.P. Xu, G.Q. Lu, Hydrothermal synthesis of layered double hydroxides (LDHs) from mixed MgO and Al<sub>2</sub>O<sub>3</sub>:  
485 LDH formation mechanism, *Chem. Mater.* 17(5) (2005) 1055-1062.

486 [58] G. Hu, N. Wang, D. O'Hare, J. Davis, Synthesis of magnesium aluminium layered double hydroxides in  
487 reverse microemulsions, *J. Mater. Chem.* 17(21) (2007) 2257.

488 [59] K.-H. Lee, S.-H. Byeon, Extended Members of the Layered Rare-Earth Hydroxide Family,  
489  $\text{RE}_2(\text{OH})_5\text{NO}_3 \cdot n\text{H}_2\text{O}$  (RE = Sm, Eu, and Gd): Synthesis and Anion-Exchange Behavior, *Eur. J. Inorg. Chem.*  
490 2009(7) (2009) 929-936.

491